processes

MDPI

Article

Size-Induced Segregation Characteristics and Phase Transition Processes of Binary Particles in Non-Cylindrical Long Rotary Drums

Chaobin Hu [1,†], Qiuhua Miao [1,2,†] and Peng Huang [2,3,*]

[1] School of Mechanical Engineering, Changshu Institute of Technology, Changshu 215500, China; superhcb@cslg.edu.cn (C.H.); qiuhua_miao@seu.edu.cn (Q.M.)
[2] School of Mechanical Engineering, Southeast University, Nanjing 211189, China
[3] State Key Laboratory of Mineral Processing Science and Technology, Beijing 102628, China
* Correspondence: huangpeng@seu.edu.cn; Tel.: +86-025-52090512
† These authors contributed equally to this work.

Abstract: In this study, the effects of drum geometric boundary conditions on size-induced segregation behaviors of binary particle systems were systematically investigated in non-cylindrical rotary drums. The results indicate that radial percolation effects and axial inclined percolation effects interact within the binary particle system in drums. In a rotary drum with a low filling rate, as the drum shape parameters change, the flow characteristics of binary particle mixtures are inconsistent, exhibiting phenomena such as the formation, reversal, splitting, merging, and replication of axial segregation bands. In contrast, with an increasing number of drum edges, rotary drums with medium filling rates gradually form axial core band characteristics with alternating intervals, while those with high filling rates gradually form axial throughout core band characteristics. Moreover, with the continuous increase in drum filling rate, the particle segregation index shows the first decrease and then increase characteristics in the final stabilization stage. Consequently, once the effects of rotary drum shape parameters and filling rate conditions are combined, the particle segregation characteristics have different phase transition processes corresponding to the different significant regions shown in the final steady segregation index phase diagrams.

Keywords: mixing and segregation; size-induced segregation; phase transition; binary particles; rotary drum

check for updates

Academic Editors: Haiping Zhu and Kaiwei Chu

Received: 20 February 2025
Revised: 17 March 2025
Accepted: 18 March 2025
Published: 25 March 2025

Citation: Hu, C.; Miao, Q.; Huang, P. Size-Induced Segregation Characteristics and Phase Transition Processes of Binary Particles in Non-Cylindrical Long Rotary Drums. *Processes* **2025**, *13*, 971. https://doi.org/10.3390/pr13040971

Copyright: © 2025 by the authors. Licensee MDPI, Basel, Switzerland. This article is an open access article distributed under the terms and conditions of the Creative Commons Attribution (CC BY) license (https://creativecommons.org/licenses/by/4.0/).

1. Introduction

Rotary drums, as typical mechanical equipment for particle drying, mixing, separation, and grinding functions, are widely used in various industrial applications such as pharmaceutical, chemical, mineral, and metallurgical industries [1,2]. Although extensive research has described particle flow behavior under varying drum geometries and operating conditions, a substantial awareness gap still exists in controlling particle segregation phenomenon [3–5]. For instance, industrial challenges directly related to particle segregation, such as particle accumulation and clogging, particle wear on critical components, and reduced product quality, need to be addressed [6,7]. Current strategies for solving these problems remain largely empirical, hence the urgency for mechanistic insights into the particle flow dynamics in rotary drums.

Currently, although different particle flow modes have been identified in rotary drums, particle mixtures with different properties often exhibit segregation rather than a complete

mixing phenomenon [8,9]. Especially existing studies have mainly focused on radial segregation in simplified short rotary drum systems, including size-induced or density-induced segregation mechanisms [10]. For example, Kawaguchi et al. [11] and Turner et al. [12] demonstrated radial core accumulation of small particles via size-induced segregation, while Pereira et al. [13] revealed the density-induced radial segregation phenomenon. Besides, Jain et al. [14] and Chen [15] et al. demonstrated that by adjusting particle size and density differences, a balance between the two segregation mechanisms can be achieved, resulting in a uniform mixture in rotating drums. Additionally, when shape differences exist, particle mixtures in rotary drums also exhibit significant flow segregation characteristics [16,17]. However, these works share two critical limitations: (a) ignoring the axial segregation patterns prevalent in industrial-scale long drums and (b) assuming idealized cylindrical geometries that do not well represent real industrial equipment subject to geometric modifications from wear or functional design. Consequently, this disparity between laboratory models and real industrial scenarios severely limits practical applicability.

Recent studies that address axial segregation in longer drums have identified key mechanisms such as wall friction effects and inclined percolation effects [18–20]. For instance, Chen and Ottino et al. [21,22] investigated the size-driven mechanism of axial segregation characteristic, pointing out that the inhomogeneous axial velocity distribution causes small particles to be moved away from the end walls, while large particles were gathered near the end walls. Besides, Cui et al. [23] found that the drum sidewall speed and friction can influence the development of axial bands, with different segregation patterns formed by competition with each other. Similarly, Arntz et al. [24,25] demonstrated that either the sidewall characteristics or the initial configuration of the drum can have an effect on axial granular band formation. Compared to particles in the middle of the drum, the additional friction of the end covers draws particles to higher positions on both sides, thus creating a slope in the axial direction. As a result, small particles undergo inclined penetration in the axial direction and move to the middle position, while large particles accumulate near the sidewalls of the drum, resulting in the axial band characteristic in the short drum. Notably, Huang et al. [26] established proportionality between drum length and axial segregation intensity, while Miao et al. [27] demonstrated opposing segregation effects of convex and concave sidewalls. Nevertheless, these studies suffer from several critical shortcomings. Specifically, oversimplified geometric models that ignore the complex non-cylindrical profiles common in industrial equipment. Besides, the interactions between drum geometry and operational parameters (e.g., filling rate) remain poorly quantified. Moreover, the existing models fail to establish phase diagrams linking geometric and operational parameters to segregation patterns.

Consequently, our work directly addresses these gaps through systematic investigation of non-cylindrical drum geometries across varying filling rates. In contrast, this study is fundamentally different from previous studies in several ways. Contrary to the work of Ayeni et al. [28], which focused on radial segregation in simple geometries, this work integrates axial dynamics segregation characterization in complex profiles of the long drums. Additionally, different from the static geometric modifications of Windows-Yule et al. [29], our work investigates the interactions between the dynamic geometric parameters. Based on these studies, it can be inferred that modifying the geometry structure of rotary drums is an effective approach for controlling radial and axial segregation patterns [30,31]. Correspondingly, the main innovations include: (a) Industrial-relevant geometric modeling: combining polygonal drum profiles and localized geometric modifications to reflect the industrial scenario drums with wear conditions. (b) Coupled parameter analysis: systematically investigating the interactions of drum geometry and filling rate on both radial and

axial segregation. (c) Phase transition framework: developing a predictive segregation index phase diagram identifying four distinct flow regimes.

The main objective of this work is to address two unresolved questions in industrial granular flows: How can the boundary conditions of non-cylindrical rotary drums be optimized to effectively enhance or suppress particle segregation behavior? And what geometric configurations and operational parameters enable optimal control of particle mixing and segregation across diverse industrial scenarios? Such investigations are critical for overcoming issues caused by particle segregation in industrial applications by optimizing structural and operational parameters. The findings provide actionable insights for equipment design and process optimization in particle-related industries, bridging the critical gap between academic models and industrial practice.

2. Numerical Method and Model Validation

2.1. Numerical Method

Compared to experimental approaches, the discrete element method (DEM), proposed by Cundall and Strack [32], can obtain information about each individual particle's motion, making it a powerful tool for studying particles. In the DEM model, the motion of spherical particles in drums can be classified into two main categories: translational motion and rotational motion. These two motions can be controlled according to Newton's second law, which can be written as [33,34]

$$m\frac{d\boldsymbol{v}}{dt} = m\boldsymbol{g} + \sum \boldsymbol{F}_c \tag{1}$$

$$I\frac{d\boldsymbol{\omega}}{dt} = \sum \boldsymbol{T}_c \tag{2}$$

in which $\boldsymbol{v}$ and $\boldsymbol{\omega}$ represent translational velocity and rotational angular velocity of the corresponding particles, respectively. I and $\boldsymbol{g}$ represent the inertia moment and the acceleration of gravity, respectively. And $\boldsymbol{F}_c$ denote the contact forces, including the normal contact forces and tangential contact forces between particles. Correspondingly, $\boldsymbol{T}_c$ represent the contact torque, including the normal and tangential torques applied to the particles. Typically, the Hertz-Mindlin (no slip) model was suitable as one of the best models for granular systems, with equations for the calculation of interaction forces and moments can be found in the literature [35–37].

To investigate the flow segregation characteristics of binary particle mixtures in the irregular rotary drums, the DEM model, which consists of non-cylindrical wall surfaces with end covers on both sides, needs to be created. In this model, the rotary drum has a length of D = 2000 mm, with specific shape and dimensions shown in Table 1. The equivalent volumes of these drums are consistent with a spherical drum with a diameter of 400 mm, including regular squares, pentagons, hexagons, octagons, dodecagons, and spheres (theoretically considered as polygons with infinite edges in the ideal case). Table 2 presents the specific DEM model parameters used in the simulation, including geometry, operating and contact parameters, with some of the model parameters referencing our previous work [26,35]. Specifically, the rotary drum was made of acrylic material, filled with green glass beads with a diameter of 6 mm and white glass beads with a diameter of 12 mm. The drum filling rate was 10~60%, and the rotational speed was 40 rpm. Note that the X direction is the drum axial direction, and the Y-Z plane is the radial view of the rotary drum (end-cover orientation view).

Table 1. Drum shapes are used in the DEM model (Equivalent area consistent with the sphere of 400 mm diameter).

Drum Shape						
Internal angle (°)	90	108	120	135	150	-
Side length (mm)	354.49	270.26	219.93	161.33	105.94	-

Table 2. DEM model parameters used in the simulation [26,35].

Parameters	**Value**	**Parameters**	**Value**
Drum diameter D (mm)	400	Drum shear modulus G (GPa)	3
Drum length	2000	Particle poisson's ratio v	0.25
Drum speed n (rpm)	40	Drum Poisson's ratio v	0.35
Drum filling rate (%)	10~60	Restitution coefficient. particle-particle	0.91/0.727
Particle volume ratio	1	Restitution coefficient. wall-particle	0.90/0.722
Particle diameter d (mm)	6/12	Static friction coeff. particle-particle	0.435
Particle density (kg/m^3)	2, 500	Static friction coeff. wall-particle	0.50
Drum density (kg/m^3)	1, 250	Rolling friction coeff. particle-particle	0.01
Particle shear modulus G (GPa)	22	Rolling friction coeff. wall-particle	0.055

In the preparatory phase of this work, the two diameter particles have the same total volume and were randomly mixed in a filled state. Besides, in order to emphasize the suitability of this DEM model, the particle flow segregation characteristics were systematically investigated in long drums with low, medium and high filling rates by varying the drum shape parameters. All DEM models were performed using the commercial software EDEM 2023 with 25% of the Rayleigh time step, running on a computer configured with an Intel i7-10700F processor, 32 GB of RAM, and an NVIDIA 3080 GPU.

2.2. Statistical Methods

Based on statistical methods, the particle segregation index in the rotary drum was quantified using the Lacey index method [38]:

$$SI = \frac{S^2 - S_r^2}{S_0^2 - {S_r}^2} \tag{3}$$

where S^2 denotes particle mixing variance in the actual mixing state. ${S_r}^2$ and ${S_0}^2$ denote particle mixing variance in the completely mixing state and completely segregated state, respectively.

For binary mixtures of two different types of particles, only a specific single type of particle is considered when evaluating the mixing and segregation degree of the particle mixtures. As shown in Figure 1, the computational domain of the rotating drum can be divided by the cubic grid in the form of $N_x \times N_y \times N_z$. For any given total number of grid samples N, the corresponding weight k_i of the sample and the total weight k can be expressed as follows

$$k_i = \frac{n_i}{n_t} \tag{4}$$

$$k = \sum_{i=1}^{N} k_i \tag{5}$$

where n_i indicates the number of particles in grid sample i, and n_t indicates the total particle number in drums. As a result, the mixed variances ${S_r}^2$, ${S_0}^2$, S^2 can be calculated from the particle number fraction as follows

$$ {S_r}^2 = \frac{P(1-P)}{n} \tag{6} $$

$$ {S_0}^2 = P(1-P) \tag{7} $$

$$ S^2 = \frac{1}{k}\sum_{i=1}^{N} k_i(a_i - \overline{a})^2 \tag{8} $$

where P indicates the proportion of one type of particle in the drum. And $(1-P)$ indicates the proportion of another type of particles in the drum. n indicates the average number of particles in each grid sample. a_i and $\overline{a}$ indicate the proportion of this type of particle in the grid sample i and in the whole drums, respectively.

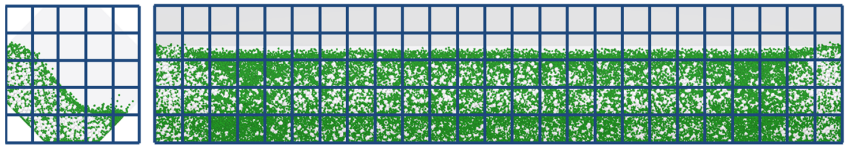


Figure 1. Meshing division of the computational domain of the rotary drum: (**a**) radial meshing division; (**b**) axial meshing division.

Notably, the Lacey index method can be divided into three steps: grid division, data extraction, and particle segregation index calculation. However, the meshing scheme has a great influence on the particle segregation index. Consequently, based on the numerical simulation for two colors of glass beads with a diameter of 12 mm, the sensitivity analysis grid sample size was performed. The total volume ratio of the two particles is 1:1, the total filling rate is 30%, and the initial structure of the filled particles is a completely segregated configuration.

Figure 2 shows the influence of grid sizes on the particle segregation index, with grid sizes set to μ = 2.0 d~μ = 5.0 d, where d represents the average equivalent diameter of binary particles. In the figure, SI = 0 represents the completely mixed state, while SI = 1.0 represents the completely segregated state. Obviously, the grid size is too large to contain sufficiently representative particle mixtures, while the grid size is too small to capture the precise mixing and segregation structure. As a result, the grid sizes of μ = 4 d can be used to quantify the mixing and segregation degree in the subsequent work, which is consistent with the work in the polydisperse particles by Wang et al. [39].

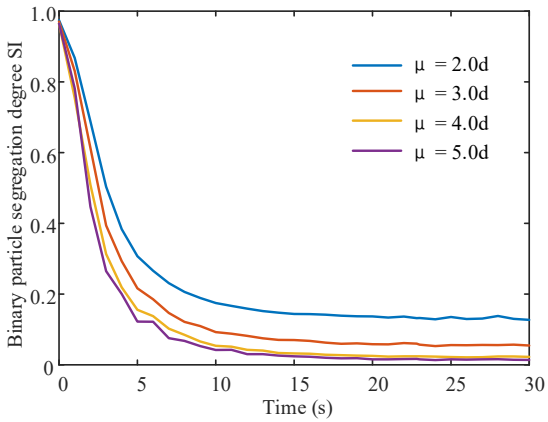


Figure 2. Sensitivity analysis of grid sizes for the segregation index of binary particle mixtures.

2.3. Model Verification

As illustrated in Figure 3, the experimental setup of the rotating drum was constructed from acrylic material, with a central cylindrical section of diameter D = 400 mm. The filled particles are white glass beads with a diameter of 12 mm and green glass beads with a diameter of 6 mm. The experimental parameters were kept consistent with those used in the DEM simulations: the two diameter particles have the same total volume, accompanied by a total drum filling rate of 10% and a drum speed of 40 rpm. Besides, three lengths of rotary drums with L = 200 mm, 400 mm, and 800 mm are selected for experiments and simulations, respectively. Once all the preparations were completed, the drum was operated at 40 rpm, and the mixing and segregation characteristics of the drum's particle mixture could be captured by the pre-set cameras. Due to the L = 800 mm drum being too long to capture a complete top view, the particle segregation patterns were recorded using a camera positioned at the radial end cover. Besides, both the experiments and simulations were repeated three times to ensure the validity of the verification.

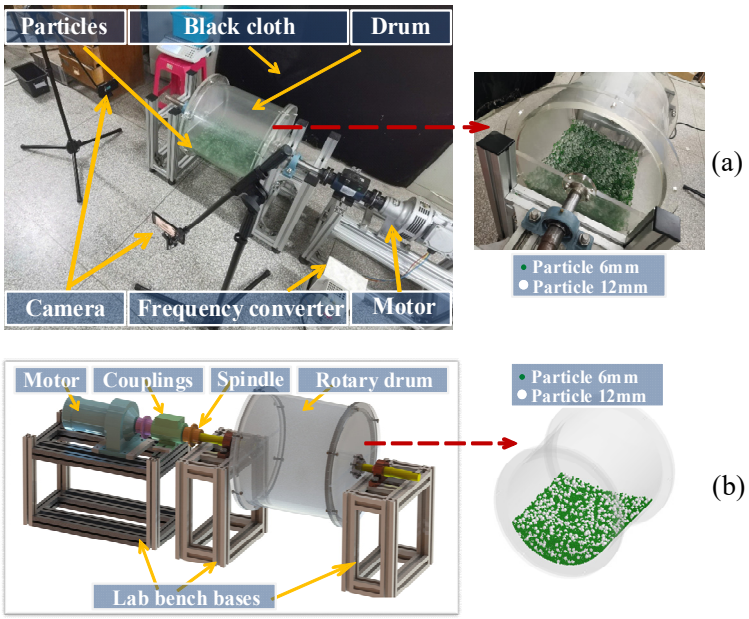


Figure 3. Experiment: (**a**) equipment set-up, (**b**) DEM model.

Figure 4 shows the surface segregation image sequence obtained in experiments and simulations, including the radial view and axial view, respectively. As illustrated in Figure 4a, in the radial view of the drum cover position, the particle trajectories and the overall dynamic repose angle in simulations are in accordance with the experimental results. During the initial lifting stage (t = 0 s to t = 0.5 s), the dynamic repose angle increased sharply from 0° to approximately 60° in both experiments and simulations. By the 5-s mark, while the overall dynamic repose angles in both cases stabilized near 26°, a distinct radial segregation pattern emerged: larger white particles began accumulating near the end cover, forming localized segregation features at the end covers. As rotation continued to t = 10 s, the dynamic repose angles were stable at about 30° in both systems. Concurrently, radial segregation intensified significantly, with smaller green particles becoming nearly undetectable at the end covers.

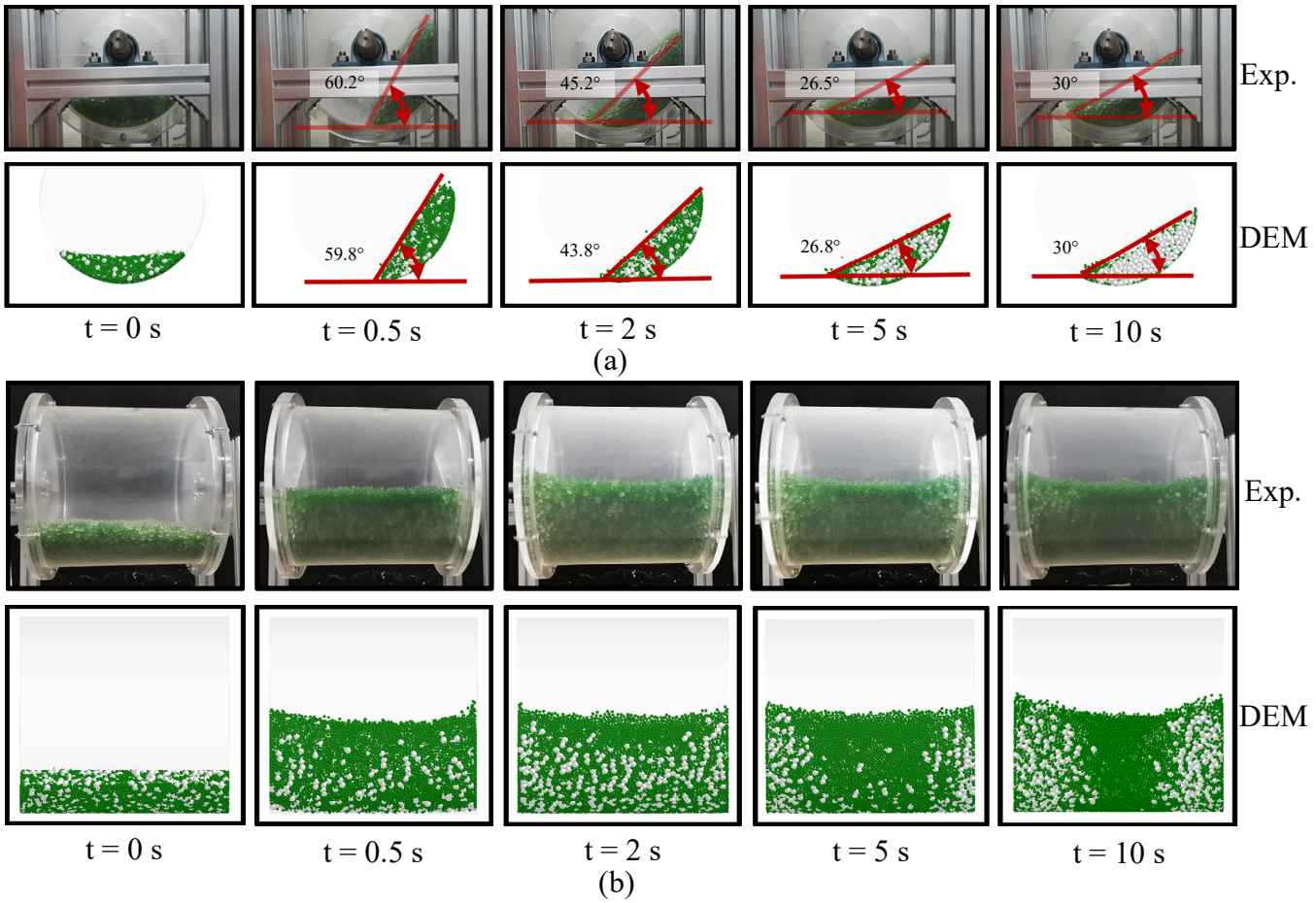


Figure 4. Segregation characteristics observed in experiments and simulations (n = 40 rpm, F = 10%): (**a**) radial view and (**b**) axial view.

Besides, Figure 4b presents the axial image sequence obtained at the axial position of the rotary drum. Notably, as the mixing process progressed, the binary particle system gradually developed a distinct axial segregation pattern. During operation, particles at the bottom of the drum are lifted and dropped along the arc-shaped trajectory induced by the drum end covers. This motion preferentially exposes larger particles on the free surface, causing them to flow back to the vicinity of both covers. Consequently, a distinct band of large particles quickly formed near both end caps, while smaller particles clustered into a central band. Moreover, combined with the DEM simulation and experimental results in Figure 4a,b, the deviation in both dynamic repose angles at different times remains below 5% in radial view. Meanwhile, in the axial view, the appearance and stabilization time of axial segregation in DEM are basically consistent with the experimental results, ensuring the validity of the contact parameters of the established DEM model.

Furthermore, Figure 5 illustrates particle segregation patterns in the final steady stage observed in both experiments and simulations. The red dashed line in the figure indicates the axial direction of the rotary drum. Obviously, the simulation results are in general agreement with the corresponding experimental results. For instance, in rotary drums with L = 200 mm and L = 400 mm, small green particles form distinct bands concentrated in the middle region, while large white particle bands are close to both sides, demonstrating the distinct axial segregation characteristics. Besides, the drum with L = 800 mm has more axial segregation bands with multiple-spaced alternating intervals. This consistency of the above results highlights the reliability of the DEM model, thereby validating the suitability for subsequent particle behavior simulations in rotary drums.

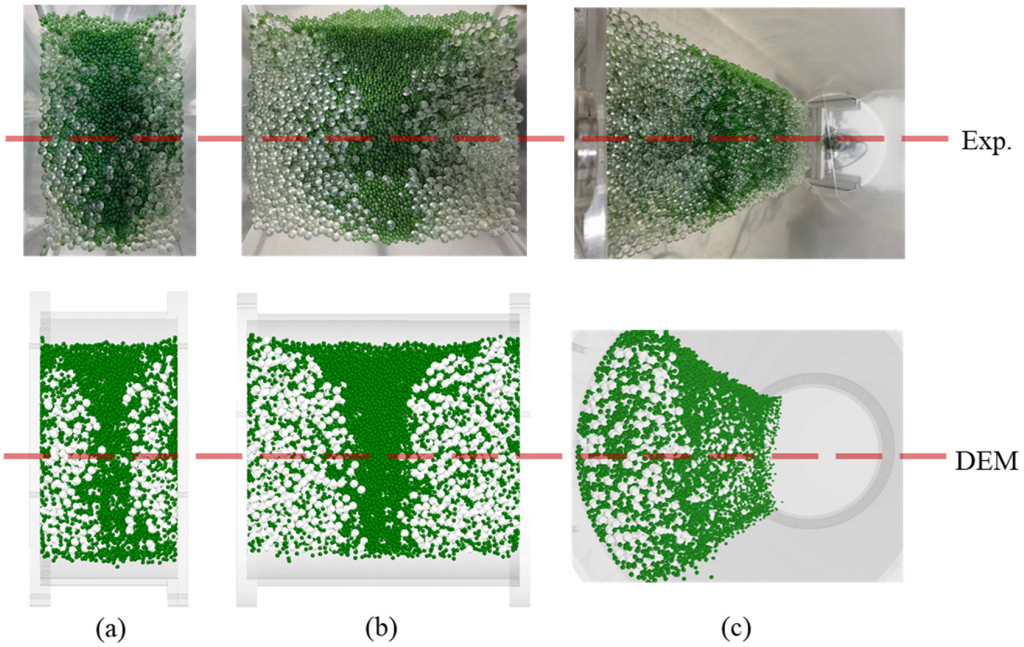


Figure 5. Steady segregation patterns observed in experiments and simulations (**a**) L = 200 mm, (**b**) L = 400 mm, (**c**) L = 800 mm.

3. Results and Discussion

In this study, the validated DEM model was employed to investigate the influence of drum shape parameters on the particle flow segregation characteristics. Specifically, six drum shapes were analyzed, all with equivalent volumes to a spherical drum of 400 mm diameter. The drum shapes encompassed a variety of regular polygons, including squares, pentagons, hexagons, octagons, dodecagons, and spheres. Besides, $F < 30\%$ and $F > 50\%$ were defined as low drum filling rate and high drum filling rate, respectively, while $30\% \leq F \leq 50\%$ was considered the medium drum filling rate. On this basis, the phase transition processes of binary particles in non-cylindrical long rotary drums, including radial and axial segregation patterns, were systematically analyzed.

3.1. Influence of Drum Shape Parameters with Low Filling Rate

In this section, six different geometric shapes were utilized to explore the influence of drum shape parameters on the particle flow segregation characteristics. In all simulations, the drum was rotated at a fixed speed of 40 rpm, and the two particles were filled with the same total volume, with different colors showing the particle segregation.

Figure 6a illustrates the axial flow segregation process in various shaped drums with a low filling rate of F = 10%. At the initial stage (t = 0 s), the binary spherical particles were almost uniformly distributed in various shaped drums with low filling rates. However, once the rotary drum rotates, the particle bed develops an inclined axial slope due to geometric constraints imposed by polygonal sidewalls and end-wall friction [27,40]. This slope triggers a size-induced inclined percolation mechanism, where smaller particles migrate toward the drum middle position while larger particles accumulate near the sidewalls, establishing axial segregation patterns. Notably, the axial segregation intensity exhibits a strong dependence on the drum side number. For example, in a square rotary drum (N = 4), relatively pure bands of small green particles and large white particles are only observed near both end covers, while the particles in the middle region remain essentially mixed without forming distinct axial bands.

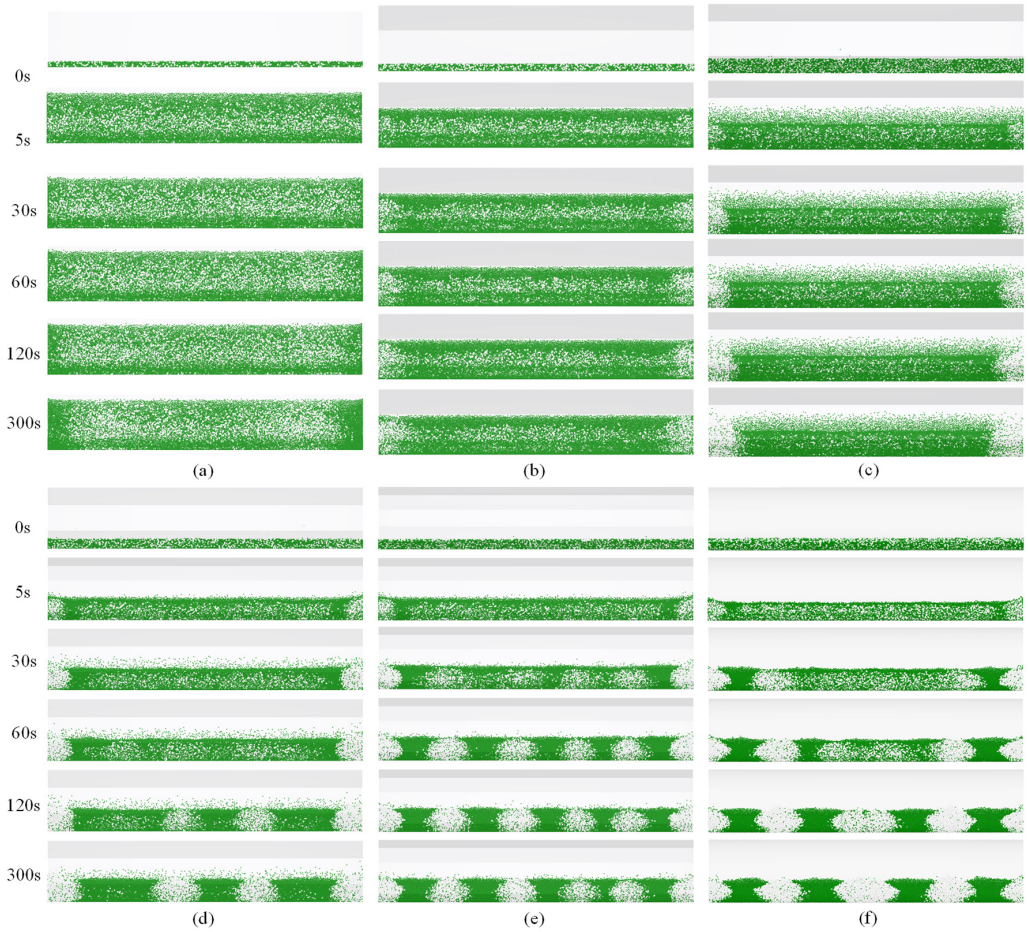


Figure 6. Flow segregation process of binary particles in various shaped drums with low filling rate (F = 10%, ω = 40 rpm, L = 2000 mm): (**a**) Square, (**b**) Pentagon, (**c**) Hexagon, (**d**) Octagon, (**e**) Dodecagon, (**f**) Cylinder (spherical surface).

In contrast, the regular pentagonal (N = 5) and hexagonal (N = 6) drums display gradually significant segregation. As the side number of the drums increases, the distinct white large-particle and green small-particle bands can be observed only at the positions near the side end caps, while the particles in the middle position remain mostly mixed without forming axial bands. Similarly, in the regular octagonal (N = 8) and dodecagonal (N = 12) drums, the insignificant axial segregation characteristic was formed at t = 5 s~t = 30 s. However, with continued rotation of the drums, the initial mixed bands in the middle position were further split and replicated into a stable axial alternating band segregation characteristic. Compared to the cylindrical drum, the number of banding segregation features is less for the regular octagonal drums, while it is more for regular dodecagonal drums.

Figure 7 systematically characterizes final particle segregation characteristics in rotating drums with various geometric configurations. The visualization employs a two-dimensional coordinate system where the vertical axis represents the drum diameter, and the horizontal axis divides the drum length into axial segments. In the particle mixing region, the particle concentration deviation was used to quantify the flow segregation characteristics, which showed that the closer the color is to yellow, the higher the proportion of large particles, and conversely, the greater the proportion of small particles. Due to the particle size effect, the size-induced binary particle system is theoretically expected to form significant axial banding segregation characteristics in drums with low particle filling rates [41,42]. However, in the regular square, pentagonal and hexagonal drums with fewer sides shown in Figure 7a–c, the mixed particles are lifted higher, resulting in a cascade

and drop state. In this case, a large number of particles collide with each other during the drop process, ultimately scattering in the middle position of the rotary drum. Moreover, observing the overall particle bed in each radial section, it was found that the morphology of the particle bed in the middle position remains basically consistent. As a result, there is essentially no difference in the dynamic angle of repose of the mixed particle bed in the middle position. Consequently, in the regular square, pentagonal, and hexagonal rotary drums, only relatively pure axial particle bands are present at both side positions, while the particles in the middle position remain in an essentially mixed state without forming alternating axial bands.

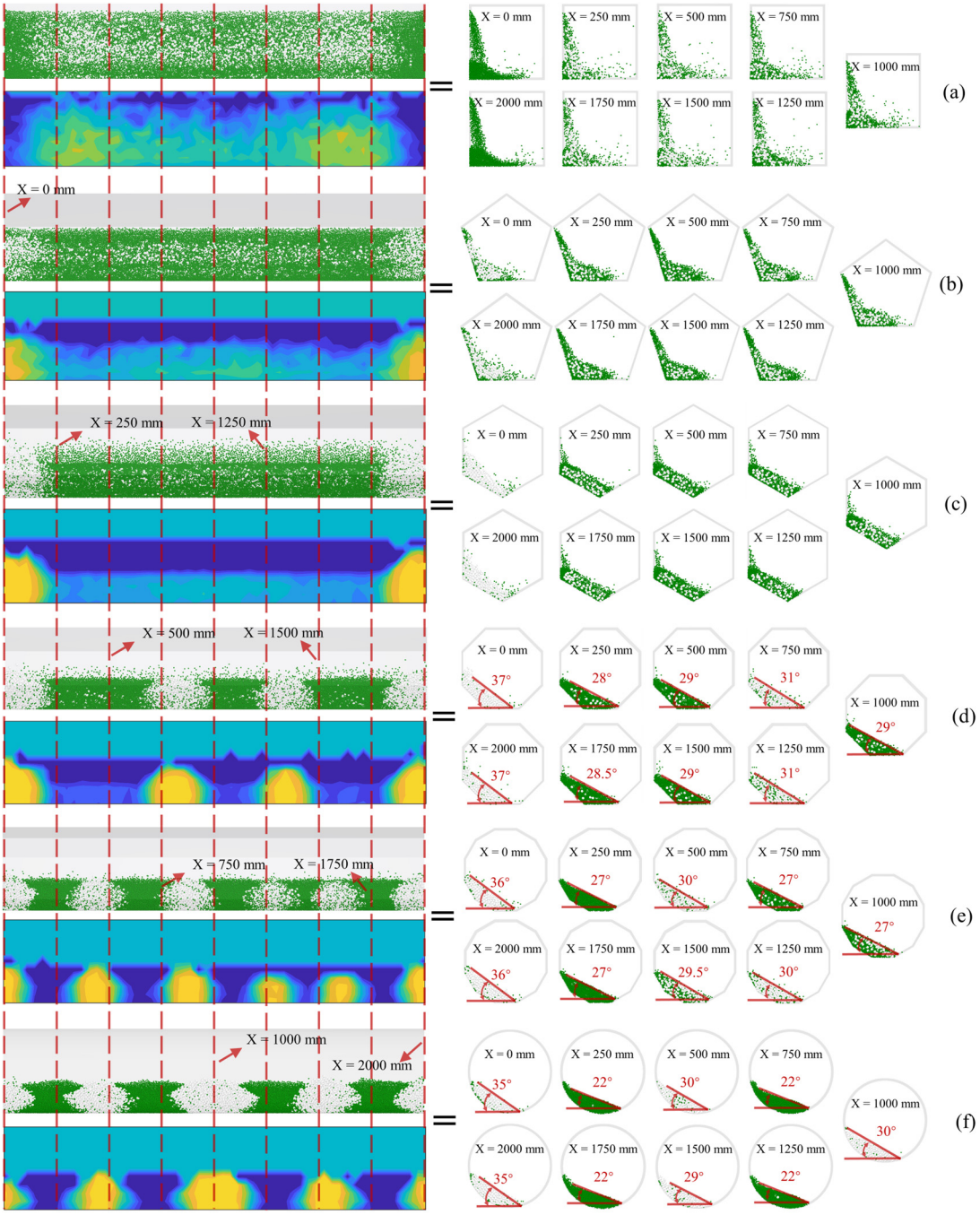


Figure 7. Final steady segregation characteristics of binary particles, including radial characteristics and axial segregation characteristics (F = 10%, t = 300 s): (**a**) Square, (**b**) Pentagon, (**c**) Hexagon, (**d**) Octagon, (**e**) Dodecagon, (**f**) Cylinder (spherical surface).

Instead, in the rotating drums with more side numbers, such as the regular octagonal and dodecagonal shapes, the mixed particles were observed to be in a constant sliding and rolling state, as shown in Figure 7d,e. Once the rotary drum continues to rotate, the overall mixed particle bed develops a significant inclined slope in the axial direction with the action of both covers. In this case, the particles in long drums undergo both radial seepage and axial inclined seepage effects due to size differences, resulting in the flow segregation phenomenon. Due to the differences in the axial dynamic repose angles of the mixed particle bed, the particles of different sizes ultimately form axial banded segregation characteristics with alternating intervals, which has been validated in the literature [23,27]. Moreover, the differences in the axial dynamic repose angles are more pronounced in the spherical rotary drum, creating more significant axial banded segregation with alternating intervals. Consequently, in the various shaped drums with low filling rates, the flow segregation characteristics of binary particles are not consistent. As the number of sides of the rotary drum increases, various phase transition phenomena related to axial segregation bands become evident, including their formation, inversion, splitting, merging, and replication. This geometric modulation of segregation patterns provides new insights for industrial drum design, suggesting that non-cylindrical profiles can intentionally suppress undesired axial segregation in low filling operations.

Additionally, Figure 8 shows the evolution of the particle segregation index in various drum shapes with low filling rates. In the F = 10% case shown in Figure 8a, the particle segregation degree is relatively low in rotary drums with fewer sides, such as regular square, pentagonal, and hexagonal shapes. As a result, the particles in these shaped drums are better mixed, making it difficult to form significant segregation structures, as verified in Figures 6 and 7. Besides, in regular square and pentagonal drums, the segregation index shows a significant sawtooth feature, which is related to the particle system being in a cascade and cataract state. In contrast, in regular pentagonal, hexagonal and even spherical drums, the segregation degree of binary particle systems is relatively higher. Correspondingly, the binary particle systems in these shaped rotary drums are sufficient to form significant segregation structures, which can also be verified in Figures 6 and 7. Similarly, in the rotary drum with a low filling rate of F = 20%, as shown in Figure 8b, although the particle segregation degree is reduced, it still increases with the number of drum sides. Compared to rotary drums with fewer sides, the segregation degree remains relatively high for drums with more than six sides.

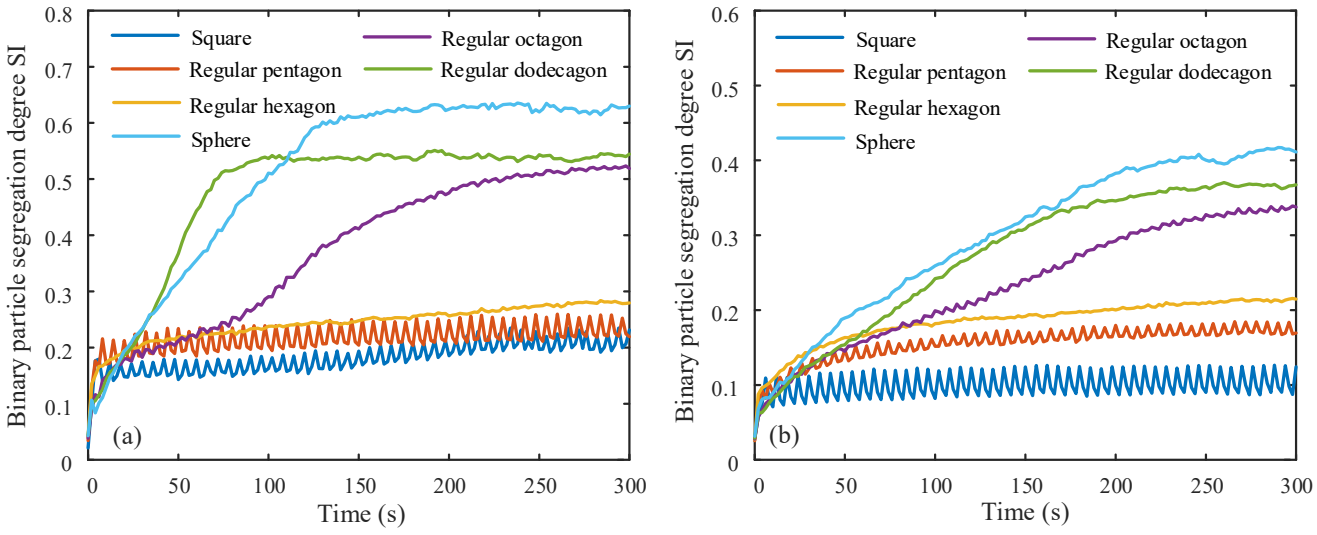


Figure 8. Segregation index evolution for binary particles in various shaped drums with low filling rate: (**a**) F = 10%, (**b**) F = 20%.

3.2. Influence of Drum Shape Parameters with Medium Filling Rate

Considering the challenge in observing segregation phenomena in drums with medium filling rates, the quantified particle concentration is projected onto an axial view to characterize the radial core characteristics and axial banded characteristics within the rotary drum. In the particle mixing region shown in Figures 9 and 10, the particle concentration deviation was used to quantify the flow segregation characteristics, which showed that the closer the color is to yellow, the higher the proportion of large particles, and conversely, the greater the proportion of small particles.

Figure 9 shows the final steady particle segregation characteristics in different-shaped drums with medium particle filling rates, including regular square, pentagonal, and hexagonal shapes. Such observations correspond to different radial sections (X = 0 mm to X = 2000 mm) in the YOZ plane of the drums, highlighting the particle distribution at different positions. Obviously, in the drum with fewer sides, the dynamic repose angle of the binary particle mixtures in the middle position is almost the same, even though it is much larger at both side positions. As a result, in these three shapes of rotary drums with medium particle filling rates, only insignificant axial core bands are characterized on both sides, while the particles in the drum middle position are still in a thoroughly mixed state. As a result, the steady segregation characteristics of the binary particles were significantly reduced in these three types of rotary drums with medium filling rates compared to those with low particle filling rates. Additionally, it was observed that the axial core band segregation characteristics at both end-cover positions increased gradually with the number of drum sides: regular square (N = 4) < regular pentagon (N = 5) < regular hexagon (N = 6).

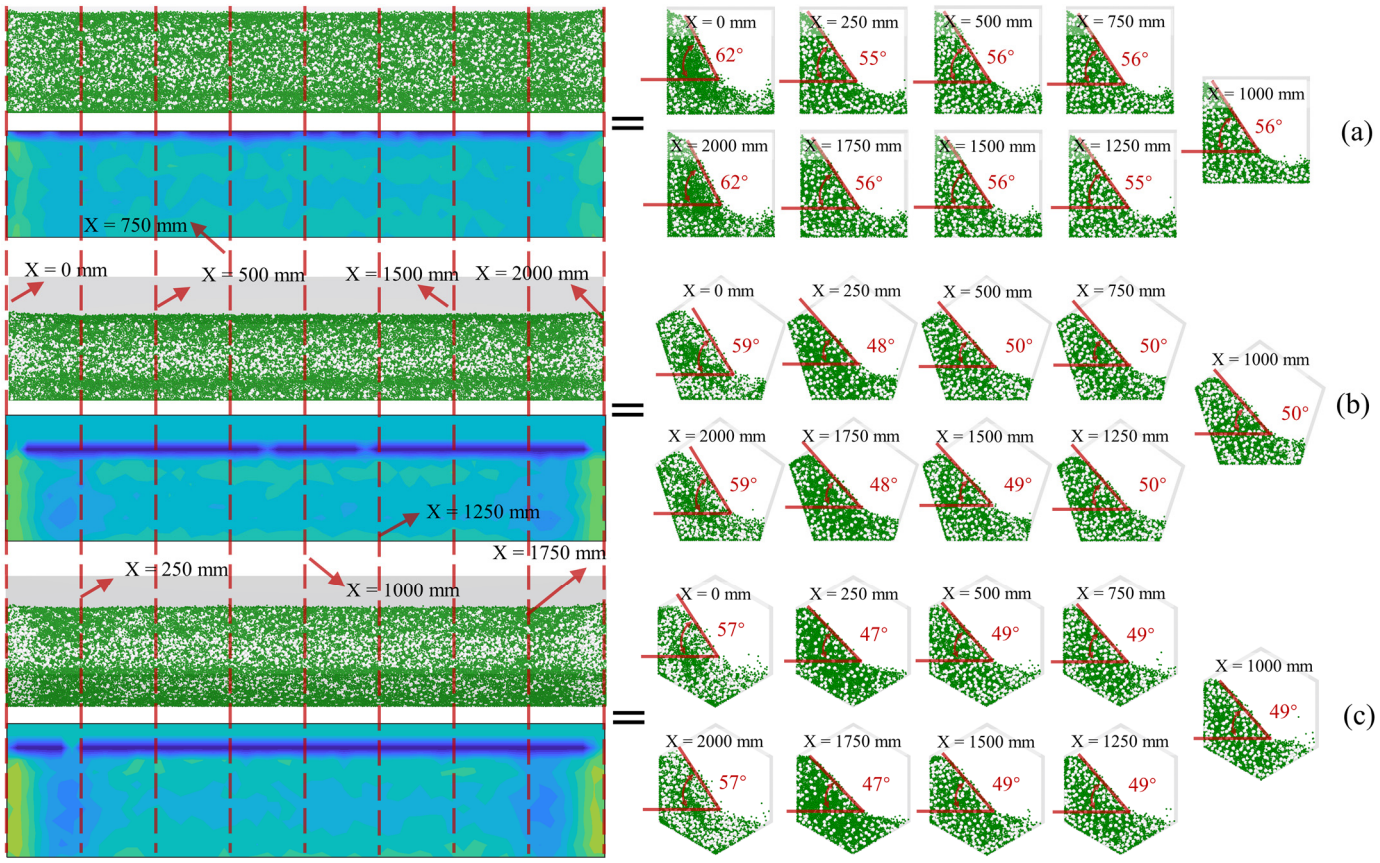


Figure 9. Final steady segregation characteristics of binary particles, including radial characteristics and axial segregation characteristics (F = 40%, t = 300 s): (**a**) Square, (**b**) Pentagon, (**c**) Hexagon.

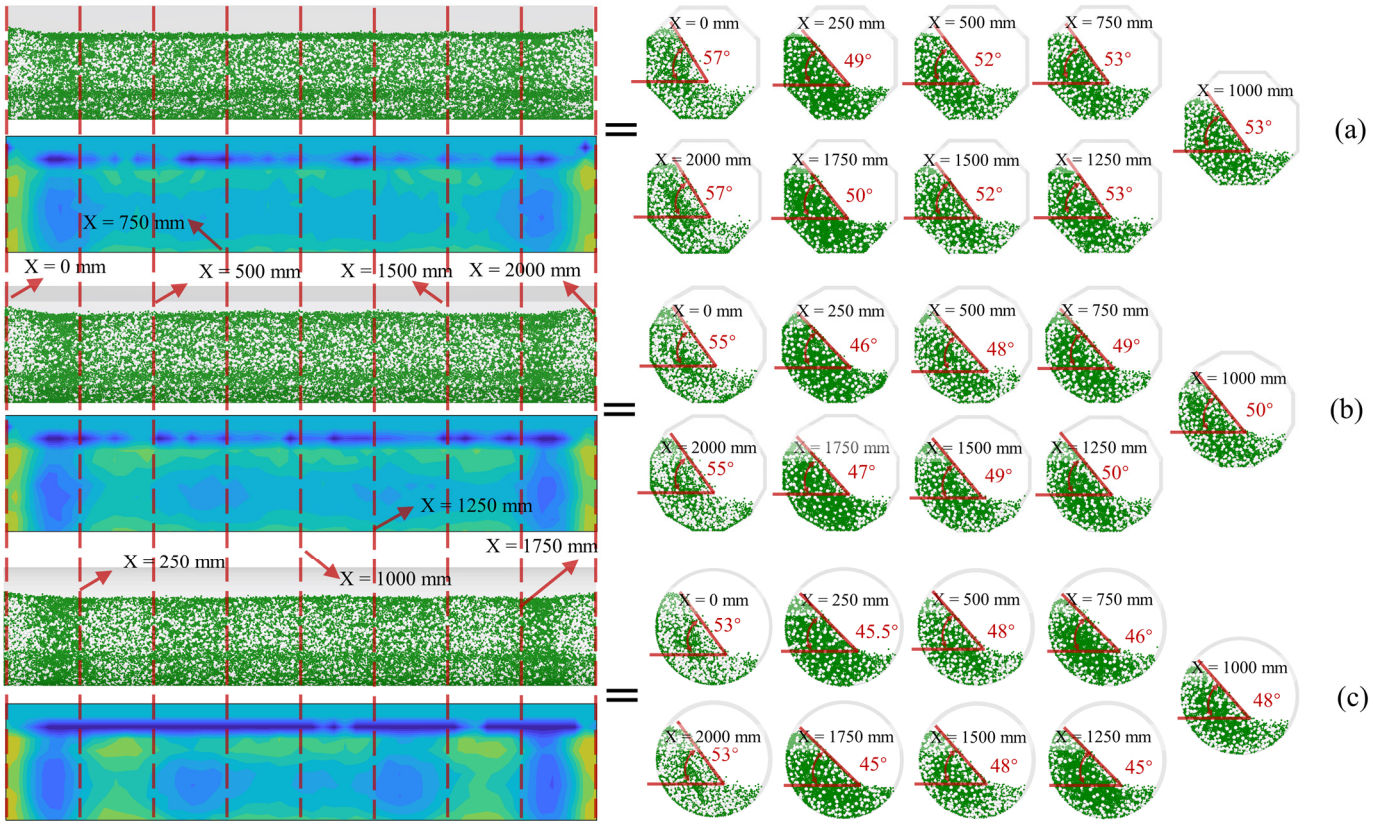


Figure 10. Final steady segregation characteristics of binary particles, including radial characteristics and axial segregation characteristics (F = 40%, t = 300 s): (**a**) Octagon, (**b**) Dodecagon, (**c**) Cylinder (spherical surface).

Figure 10 shows the final steady particle segregation characteristics in the remaining shapes of the long drum, including regular octagonal, dodecagonal, and cylinder surfaces. Evidently, the inclined slope of the free surface of the overall particle bed increases with the side number of the rotating drums. In this case, the particle mixture has two flow segregation effects in the radial and axial directions, i.e., the radial seepage effect and the axial inclined seepage effect compete with each other. Besides, in drums with larger side numbers, such as the regular dodecagonal and cylinder shapes, the dynamic repose angle of the particles is also characterized by an interval distribution in the middle of the drum, even though the dynamic angle of repose at both sides is much larger. As a result, in these three shapes of rotary drums with medium particle filling rates, the pure axial core bands are characterized at both sides, while the axial core band characteristics with alternating intervals are gradually developed in the middle position. Consequently, with the increase in the number of sides of the rotary drum, the axial core band characteristics with alternating intervals are gradually developed in the medium filling rate rotary drum. Especially in rotary drums with larger side numbers, i.e., regular dodecagonal and cylinder shapes, such axial core band characteristics with alternating intervals are very noticeable.

In addition, Figure 11 plots the particle segregation index evolution in rotary drums with the medium filling rates. On the whole, compared to low drum filling conditions, the segregation index in various shaped drums with medium particle filling rate decreases significantly. Specifically, in the F = 40% case, the particle segregation degree is significantly low in rotary drums with fewer edges, such as regular square (N = 4), pentagonal (N = 5), and hexagonal (N = 6) shaped drums. As a result, the binary particle systems in these shaped drums are better mixed, and it is difficult to form significant segregation structures, which can be verified in Figure 9. In contrast, in rotary drums with more side numbers,

e.g., regular octagonal (N = 8), dodecagonal (N = 12), or even spherical (N = ∞) drums, the particle segregation degree is relatively high. Accordingly, the binary particle systems in these shaped drums are sufficient to form significant flow segregation structures, which can be verified in axial core band characteristics with alternating intervals in Figure 10. Consequently, in the medium filling rate cases, the segregation characteristics are not consistent as the drum shape parameters vary. Notably, with the increase in the number of sides of the rotary drum, the significant axial core band features with alternating intervals gradually developed in rotary drums.

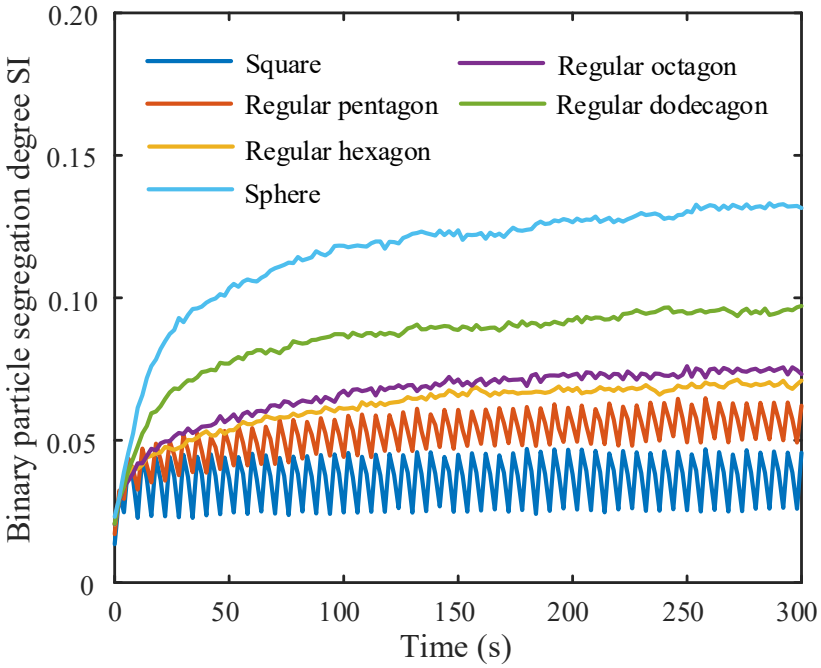


Figure 11. Particle segregation index in various shaped drums with medium particle filling rate (F = 40%).

3.3. Influence of Drum Shape Parameters with High Filling Rate

Considering the challenge in observing segregation phenomena in drums with high filling rates, the quantified particle concentration is projected onto an axial view to characterize the radial core characteristics and axial banded characteristics within the rotary drum. Figures 12 and 13 show the final segregation characteristics for differently shaped drums with high filling rates, respectively. In the particle mixing region shown in Figures 12 and 13, the particle concentration deviation was used to quantify the flow segregation characteristics, which showed that the closer the color is to yellow, the higher the proportion of large particles, and conversely, the greater the proportion of small particles.

In long drums with fewer sides, as shown in Figure 12, although the dynamic repose angle of the particle mixtures on both sides is much larger, it shows minimal differences in the middle of the drum. As a result, in these three shapes of rotary drums with high particle filling rates, only significant axial core band features were formed on both sides of the drums. However, compared to the drums with low and medium particle filling rates, single axial-through core band features are gradually formed in the drums with high particle filling rates.

Besides, in rotary drums with more sides, as illustrated in Figure 13, the binary particles develop a significant axial inclined slope under the end-cover effects that intensify with polygonal complexity. This configuration induces dual segregation mechanisms: the radial seepage effect and the axial inclined seepage effect. Although the dual segregation

mechanisms coexist in all configurations, compared to the low and medium filling rate drums, the radial seepage effect plays a key role in the high filling rate drums. Especially with the increase in the number of sides of the rotary drum, the significant axial-through core band characteristics were gradually formed in drums with high filling rates. Especially in the regular dodecagonal and spherical drums, quite significant axial-through core band characteristics can be observed.

As demonstrated in Figure 14, the particle segregation index evolution at high filling rates shows a distinct geometric dependence. Contrary to the medium filling rate cases, the high filling rate cases exhibit amplified segregation indices, with polygonal geometry critically modulating segregation intensity. Specifically, the square drum (lowest polygonal complexity) demonstrated the weakest segregation intensity, while polygonal geometries with more sides (e.g., hexagonal, octagonal) showed progressive enhancement. This trend confirms radial seepage effects as the dominant segregation mechanism in high filling systems, which is also verified in in the axial core band characterization in Figure 13. Consequently, once the shape of a drum with a high filling rate was changed, the radial segregation and axial segregation characteristics were not uniform. With the increase in the side number of the rotary drum, significant axial-through core band characteristics gradually developed in high filling rate cases.

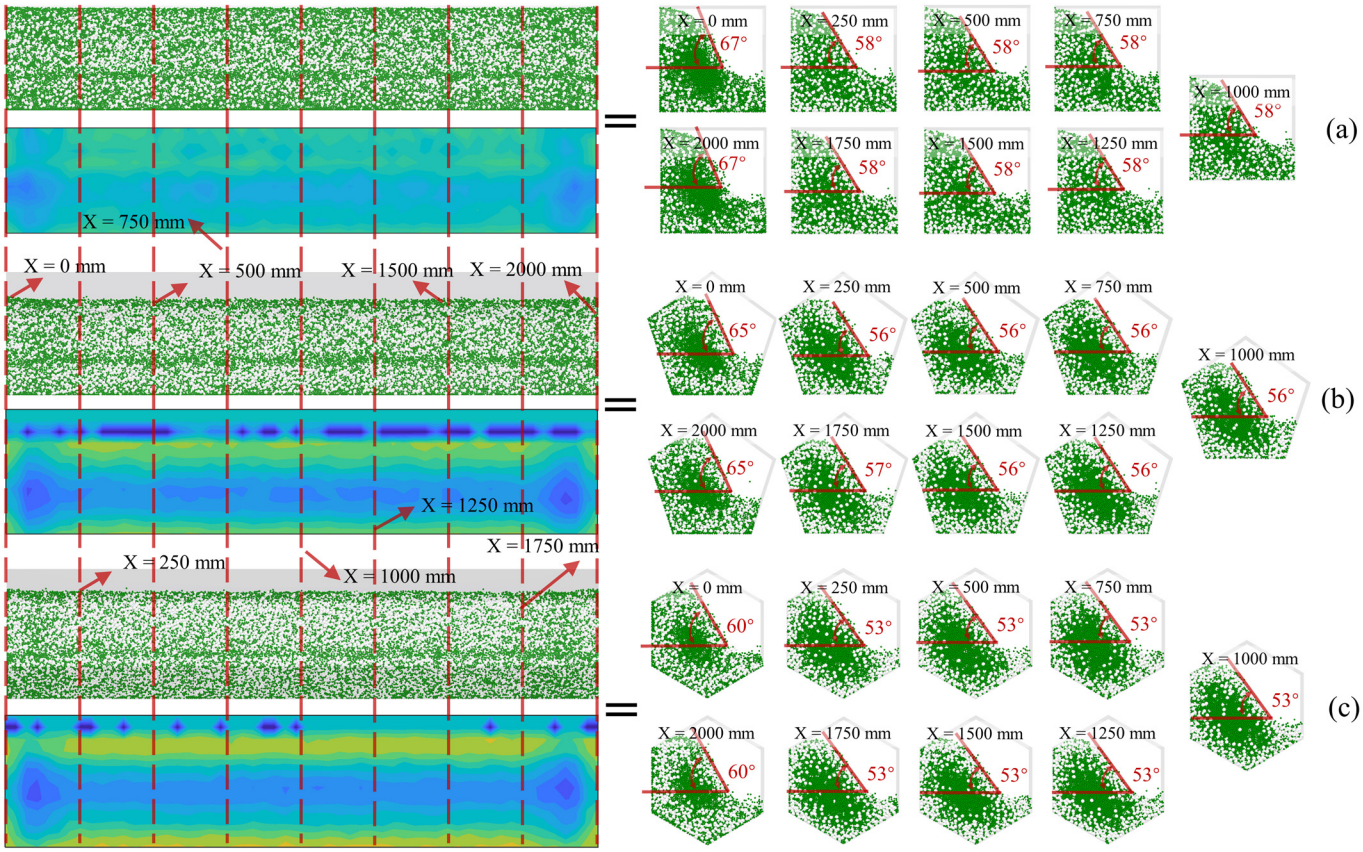


Figure 12. Final steady segregation characteristics of binary particles, including radial characteristics and axial segregation characteristics (F = 60%, t = 300 s): (**a**) Square, (**b**) Pentagon, (**c**) Hexagon.

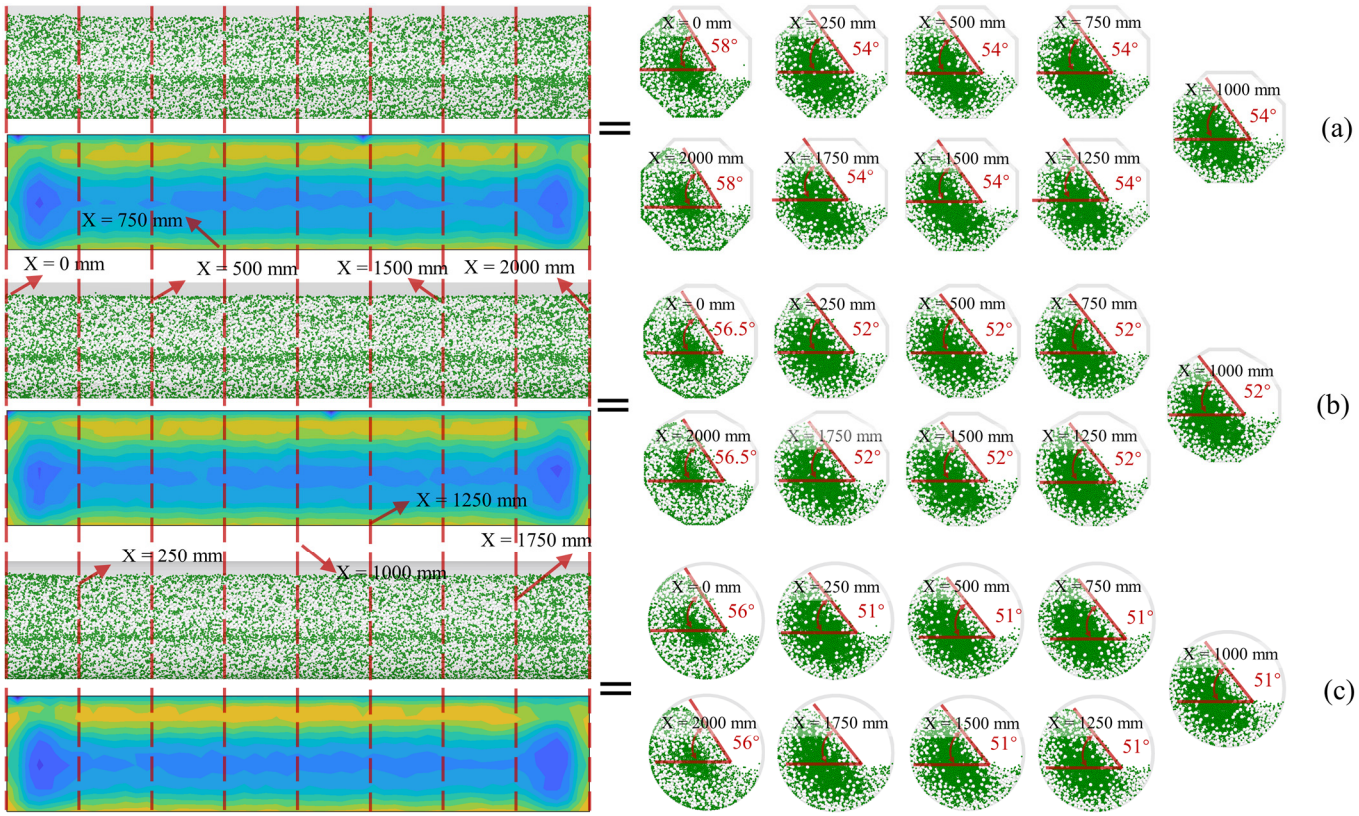


Figure 13. Final steady segregation characteristics of binary particles, including radial characteristics and axial segregation characteristics (F = 60%, t = 300 s): (**a**) Octagon, (**b**) Dodecagon, (**c**) Cylinder (spherical surface).

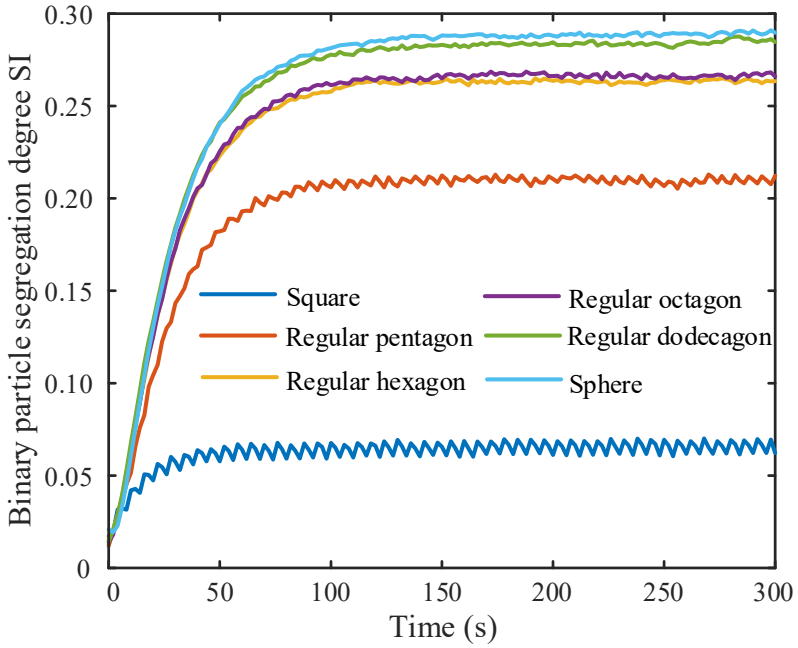


Figure 14. Segregation index evolution for binary particles in various shaped drums with medium particle filling rate (F = 60%).

3.4. Combined Effect of Drum Shape Parameters and Drum Filling Rate

Figure 15 illustrates the final steady segregation characteristics under parametric modulation of drum geometry and drum filling rates. Obviously, the system exhibits a

mechanistic competition between the radial seepage effect and the axial inclined seepage effect, with dominance governed by operational parameters. On the one hand, the geometric configuration of the rotary drum (increasing side number) systematically shifts the balance toward an axial inclined seepage effect, inducing complex morphological transformations in banded segregation patterns, which include axial band formation, band inversion, band splitting and fusion, as well as spatial replication of axial bands. On the other hand, with the increase in drum filling rate, the radial seepage effect gradually plays a key role, contributing to the gradual enhancement in the axial core band segregation characteristics. Especially in drums with high filling rates, the binary particle system is specifically characterized by the axial-through core band segregation features with a dark blue color. This parametric duality reveals a key drum geometry-drum filling rate coupling relationship, manifested in the fact that the drum geometry determines the selection of the axial segregation band characteristics, while the drum filling rate determines the scaling of the radial segregation core characteristics.

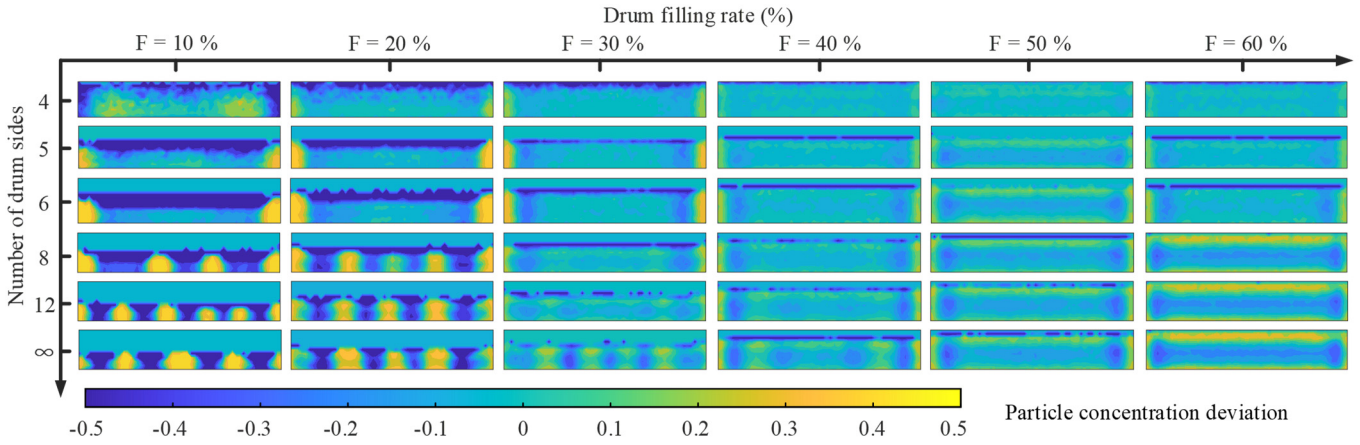


Figure 15. Axial projection of the final steady segregation characteristics considering the combined effect of drum shapes and filling rates.

Moreover, Figure 16 demonstrates the combined effect based on the final steady segregation index phase diagram. Firstly, from the perspective of the horizontal axis in the phase diagram, the steady segregation degree of binary particles shows the first decreasing and then increasing characteristics with the increasing drum filling rates. It is consistent with the phase transition process of flow segregation characteristics in drums with different filling rates. In addition, from the perspective of the vertical axis in the phase diagram, the final steady segregation index of the binary particles exhibits a continuous increase characteristic with the continuous increase in the number of sides of the rotating drum. It is also consistent with the continuous enhancement of the flow segregation characteristics with the increasing number of drum sides.

As a result of the combined effect of drum shapes and filling rates, the binary particles' mixing and segregation characteristics have four phase transition processes corresponding to final steady segregation index phase diagrams showing four significant flow segregation characteristic regions, respectively. Despite the existence of phase transition processes in binary particle flow segregation characteristics, the indices of these segregation characteristics generally follow a decreasing trend and can be divided into the following regions: (I) axial band segregation characteristics with alternating intervals, (II) axial-through core band characteristics, (III) axial core band characteristics with alternating intervals, (IV) none segregation characteristic (almost mixed state). Therefore, with the adjustment of drum shapes and filling rates, such a phase transition process reveals the significant influence of drum shape parameters and operational conditions on particle mixing and segregation behavior.

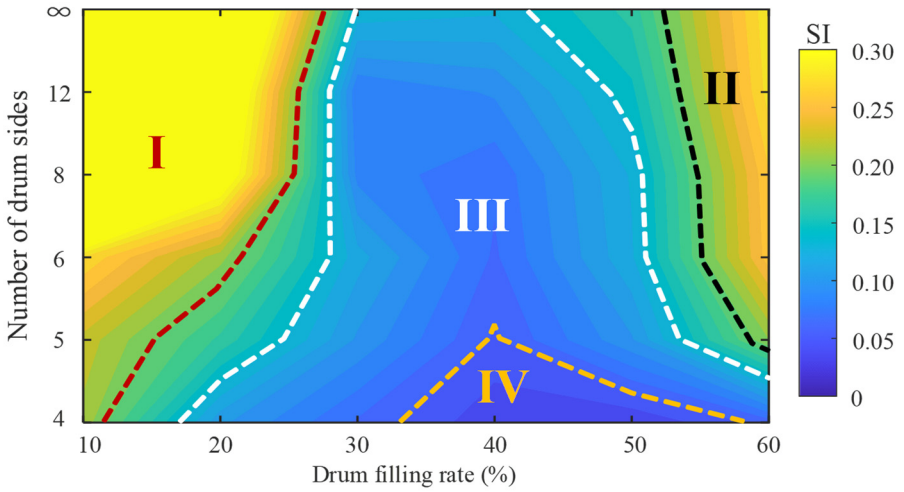


Figure 16. The final steady segregation index of binary particles considers the combined effect of drum shapes and drum filling rates.

4. Conclusions

In this work, the radial and axial segregation characteristics of binary particles are investigated by varying the drum shape and filling rate conditions. Based on the quantitative particle segregation degree, the evolution of the particle segregation pattern is analyzed. The following conclusions can be summarized from the results:

(1) In low drum filling rate conditions, once the drum shapes are changed, the binary particles suffer from the formation, inversion, splitting, merging, and replication of axial banded segregation characteristics.

(2) With the increase in the drum filling rates, the final stead segregation index of binary particles shows the first decreasing and then increasing characteristics. In particular, axial band segregation characteristics with alternating intervals are gradually formed in drums with medium filling rates, whereas axial-through core band characteristics are gradually formed in drums with high filling rates.

(3) With the increase in the number of drum sides, the axial inclined seepage effect gradually plays a key role, which is characterized by a continuous increase in the final steady segregation index of binary particles.

(4) With the combined effect of drum shapes and drum filling rates, the flow segregation of binary particles in rotary drums can be characterized by four phase transitions corresponding to the different mixing and segregation regions in the segregation index phase diagram, respectively.

The findings of this study have significant implications for industries relying on granular material processing, including pharmaceuticals, agriculture, and mining. However, addressing these challenges will require further research, such as pilot-scale experiments and computational modeling tailored to specific industrial applications. By bridging the gap between laboratory findings and industrial practice, further groundwork is laid to advance particle material processing technology. Having said that, the current work assumes idealized particle properties and does not account for factors commonly encountered in industrial settings, such as particle cohesion, moisture, or non-uniform size distributions. Correspondingly, future research could explore these factors to enhance the model's applicability to industrial scenarios and enhance operational efficiency in industrial processes.

Author Contributions: Conceptualization, C.H.; Methodology, Q.M.; Software, C.H. and P.H.; Validation, C.H. and Q.M.; Formal analysis, C.H.; Investigation, Q.M.; Resources, P.H.; Writing—original

draft preparation, Q.M.; Writing—review and editing, C.H. and Q.M.; Supervision, P.H.; Funding acquisition, C.H. and P.H. All authors have read and agreed to the published version of the manuscript.

Funding: This research was funded by the Jiangsu Key Laboratory for Elevator Intelligent Safety, grant number JSKLESS202105, Open Foundation of State Key Laboratory of Mineral Processing Science and Technology, grant number BGRIMM-KJSKL-2024-21, and China Scholarship Council, grant number 202306090115.

Data Availability Statement: The data presented in this study are available on request from the corresponding author.

Conflicts of Interest: The authors declare no conflicts of interest.

References

1. Li, G.; Zhang, H.; Ye, X.; Su, Y.; Yu, A.; Tan, Y. Numerical Investigation on Thermal Drying Process of Sludges Based on CFD-DEM. *Ind. Eng. Chem. Res.* **2023**, *62*, 16990–17007. [CrossRef]
2. Zhao, Y.; Zhang, L.; Song, C.; Li, W.; Qin, H.; Wang, Q. Numerical Simulations of Particle Motions at Continuous Rotational Speed Changes in Horizontal Rotating Drums. *Processes* **2023**, *11*, 47. [CrossRef]
3. Kreesaeng, S.; Chalermsinsuwan, B.; Piumsomboon, P. Effect of Inserting Baffles on the Solid Particle Segregation Behavior in Fluidized Bed Reactor: A Computational Study. *ChemEngineering* **2024**, *8*, 7. [CrossRef]
4. Adepu, M.; Chen, S.; Jiao, Y.; Gel, A.; Emady, H. Wall to Particle Bed Contact Conduction Heat Transfer in a Rotary Drum Using DEM. *Comp. Part. Mech.* **2021**, *8*, 589–599. [CrossRef]
5. He, S.; Wang, Y.; Zhou, Z.; Gan, J.; Yu, A.; Pinson, D. Size-Induced Axial Segregation of Ellipsoids in a Rotating Drum. *Powder Technol.* **2023**, *422*, 118490. [CrossRef]
6. Li, M.; An, X.; Wu, Y. Segregation Behavior of Particles with Gaussian Distributions in the Rotating Drum with Rolling Regime. *Adv. Powder Technol.* **2023**, *34*, 103953. [CrossRef]
7. Ahmed, E.M.E.; Govender, I.; Mainza, A.N. Axial Segregation of Polydisperse Granular Mixtures in Rotating Drum Flows. *Minerals* **2021**, *11*, 915. [CrossRef]
8. Mesnier, A.; Peczalski, R.; Mollon, G.; Vessot-Crastes, S. Mixing of Bi-Dispersed Milli-Beads in a Rotary Drum. Mechanical Segregation Analyzed by Lab-Scale Experiments and DEM Simulation. *Processes* **2020**, *8*, 1166. [CrossRef]
9. Yang, L.Y.M.; Zheng, Q.J.; Bai, L.; Yu, A.B. Continuum Modelling of Granular Segregation by Coupling Flow Rheology and Transport Equation. *Powder Technol.* **2021**, *378*, 371–387. [CrossRef]
10. Naji, L.; Stannarius, R. Axial and Radial Segregation of Granular Mixtures in a Rotating Spherical Container. *Phys. Rev. E* **2009**, *79*, 031307. [CrossRef]
11. Kawaguchi, T.; Tsutsumi, K.; Tsuji, Y. MRI Measurement of Granular Motion in a Rotating Drum. In Proceedings of the Particle and Particle Systems Characterization; Wiley Online Library: Hoboken, NJ, USA, 2006; Volume 23, pp. 266–271.
12. Turner, J.L.; Nakagawa, M. Particle Mixing in a Nearly Filled Horizontal Cylinder through Phase Inversion. *Powder Technol.* **2000**, *113*, 119–123. [CrossRef]
13. Pereira, G.G.; Sinnott, M.D.; Cleary, P.W.; Liffman, K.; Metcalfe, G.; Šutalo, I.D. Insights from Simulations into Mechanisms for Density Segregation of Granular Mixtures in Rotating Cylinders. *Granul. Matter* **2011**, *13*, 53–74. [CrossRef]
14. Jain, N.; Ottino, J.M.; Lueptow, R.M. Regimes of Segregation and Mixing in Combined Size and Density Granular Systems: An Experimental Study. *Granul. Matter* **2005**, *7*, 69–81. [CrossRef]
15. Chen, H.; Zhao, X.; Xiao, Y.; Liu, Y.; Liu, Y. Radial Mixing and Segregation of Granular Bed Bi-Dispersed Both in Particle Size and Density within Horizontal Rotating Drum. *Trans. Nonferrous Met. Soc. China* **2016**, *26*, 527–535. [CrossRef]
16. Cleary, P.W.; Morrison, R.D. Comminution Mechanisms, Particle Shape Evolution and Collision Energy Partitioning in Tumbling Mills. *Miner. Eng.* **2016**, *86*, 75–95. [CrossRef]
17. Jo, S.-A.; Kim, E.-K.; Cho, G.-C.; Lee, S.-W. Particle Shape and Crushing Effects on Direct Shear Behavior Using DEM. *Soils Found.* **2011**, *51*, 701–712. [CrossRef]
18. Zuo, Z.; Wang, J.; Wu, X.; Gong, S.; Zhang, J.; Lu, X. Segregation Dynamics of the Binary-Size Granular System in a Split Rotary Drum. *Powder Technol.* **2022**, *404*, 117480. [CrossRef]
19. Zuo, Z.; Wang, J.; Chen, X.; Gong, S.; Lu, H. Numerical Study of Forced Axial Segregation of Binary Density Granular System in a Split Rotary Drum. *Adv. Powder Technol.* **2022**, *33*, 103831. [CrossRef]
20. Das Gupta, S.; Khakhar, D.V.; Bhatia, S.K. Axial Segregation of Particles in a Horizontal Rotating Cylinder. *Chem. Eng. Sci.* **1991**, *46*, 1513–1517. [CrossRef]
21. Chen, P.; Lochman, B.J.; Ottino, J.M.; Lueptow, R.M. Inversion of Band Patterns in Spherical Tumblers. *Phys. Rev. Lett.* **2009**, *102*, 148001. [CrossRef]

22. Chen, P.; Ottino, J.M.; Lueptow, R.M. Onset Mechanism for Granular Axial Band Formation in Rotating Tumblers. *Phys. Rev. Lett.* **2010**, *104*, 188002. [CrossRef] [PubMed]
23. Cui, Z.; Zhao, Y.; Chen, Y.; Liu, X.; Hua, Z.; Zhou, C.; Zheng, J. Transition of Axial Segregation Patterns in a Long Rotating Drum. *Particuology* **2014**, *13*, 128–133. [CrossRef]
24. Arntz, M.M.H.D.; den Otter, W.K.; Beeftink, H.H.; Boom, R.M.; Briels, W.J. The Influence of End Walls on the Segregation Pattern in a Horizontal Rotating Drum. *Granul. Matter* **2013**, *15*, 25–38. [CrossRef]
25. Arntz, M.M.H.D.; Beeftink, H.H.; den Otter, W.K.; Briels, W.J.; Boom, R.M. Segregation of Granular Particles by Mass, Radius, and Density in a Horizontal Rotating Drum. *AIChE J.* **2014**, *60*, 50–59. [CrossRef]
26. Huang, P.; Miao, Q.; Ding, Y.; Sang, G.; Jia, M. Research on Surface Segregation and Overall Segregation of Particles in a Rotating Drum Based on Stacked Image. *Powder Technol.* **2021**, *382*, 162–172. [CrossRef]
27. Miao, Q.; Zhu, W.; Cao, Y.; Huang, P.; Hu, C.; Jia, M. Axial Segregation Characteristics and Size-Induced Flow Behavior of Particles in a Novel Rotary Drum with Curved Sidewalls. *Particuology* **2024**, *87*, 1–19. [CrossRef]
28. Ayeni, O.O.; Wu, C.L.; Joshi, J.B.; Nandakumar, K. A Discrete Element Method Study of Granular Segregation in Non-Circular Rotating Drums. *Powder Technol.* **2015**, *283*, 549–560. [CrossRef]
29. Windows-Yule, C.R.K.; van der Horn, A.J.; Tunuguntla, D.R.; Parker, D.J.; Thornton, A.R. Inducing Axial Banding in Bidisperse-by-Density Granular Systems Using Noncylindrical Tumbler Geometries. *Phys. Rev. Appl.* **2017**, *8*, 024010. [CrossRef]
30. Cleary, P.W. Predicting Charge Motion, Power Draw, Segregation and Wear in Ball Mills Using Discrete Element Methods. *Miner. Eng.* **1998**, *11*, 1061–1080. [CrossRef]
31. Xie, C.; Zhao, Y.; Song, T.; Zhao, Y. Investigation of the Effect of Filling Level on the Wear and Vibration of a SAG Mill by DEM. *Particuology* **2022**, *63*, 24–34. [CrossRef]
32. Cundall, P.A.; Strack, O.D.L. A Discrete Numerical Model for Granular Assemblies. *Geotechnique* **1979**, *29*, 47–65. [CrossRef]
33. Yu, F.; Zhang, S.; Zhou, G.; Zhang, Y.; Ge, W. Geometrically Exact Discrete-Element-Method (DEM) Simulation on the Flow and Mixing of Sphero-Cylinders in Horizontal Drums. *Powder Technol.* **2018**, *336*, 415–425. [CrossRef]
34. Rong, W.; Li, B.; Feng, Y. The Development and Application of a TFM for Dense Particle Flow and Mixing in Rotating Drums. *Processes* **2022**, *10*, 234. [CrossRef]
35. Miao, Q.; Huang, P.; Ding, Y.; Guo, J.; Jia, M. Particle mixing and segregation behaviors in the rotating drums with adjacent axial segmentations in different speed directions. *Powder Technol.* **2022**, *405*, 117534. [CrossRef]
36. Zhou, Y.C.; Wright, B.D.; Yang, R.Y.; Xu, B.H.; Yu, A.B. Rolling Friction in the Dynamic Simulation of Sandpile Formation. *Phys. A Stat. Mech. Its Appl.* **1999**, *269*, 536–553. [CrossRef]
37. Ai, J.; Chen, J.-F.; Rotter, J.M.; Ooi, J.Y. Assessment of Rolling Resistance Models in Discrete Element Simulations. *Powder Technol.* **2011**, *206*, 269–282. [CrossRef]
38. Lacey, P.M.C. The Mixing of Solid Particles. *Chem. Eng. Res. Des.* **1997**, *75*, S49–S55. [CrossRef]
39. Wang, S.; Zhou, Z.; Ji, S. Radial Segregation of a Gaussian-Dispersed Mixture of Superquadric Particles. *Powder Technol.* **2021**, *394*, 813–824. [CrossRef]
40. Jain, A.; Evrard, F.; van Wachem, B. The Effect of Side Walls on Particles Mixing in Rotating Drums. *Particuology* **2023**, *72*, 112–121. [CrossRef]
41. Huang, P.; Miao, Q.; Sang, G.; Zhou, Y.; Jia, M. Research on Quantitative Method of Particle Segregation Based on Axial Center Nearest Neighbor Index. *Miner. Eng.* **2021**, *161*, 106716. [CrossRef]
42. Miao, Q.; Cao, Y.; Zhu, W.; Huang, P.; Huang, L.; Yu, A.; Kuang, S. Segregation Flow Behavior of Polydisperse Particle Mixture with Skewed Distribution in a Rotating Drum. *Powder Technol.* **2024**, *444*, 120041. [CrossRef]

Disclaimer/Publisher's Note: The statements, opinions and data contained in all publications are solely those of the individual author(s) and contributor(s) and not of MDPI and/or the editor(s). MDPI and/or the editor(s) disclaim responsibility for any injury to people or property resulting from any ideas, methods, instructions or products referred to in the content.